Electronegative Gas Doping to Improve Energy Resolution in Time Projection Chamber Detectors

Drew Gibson

Advisor: Dr. Dinesh Loomba

Rare event searches require increasingly strict bounds on energy resolution to aid in the detection of events. A method of improving energy resolution in time projection chamber (TPC) detectors involves introducing electronegative gases to count the individual primary ionization electrons. This has been shown to work by another group, but they did not achieve the theoretical limit of $< 1\%$ energy resolution. Our detector will be able to continue studies into this method by testing new gas mixtures in an attempt to continue lowering the energy resolution threshold.

1 Introduction

Rare event searches are a sector of physics experimentation that requires exquisite spatial and energy resolution in the detectors utilized. Due to the low expected rate, every potential event in the detector is crucial for the analysis. Any loss of events could be detrimental to the overall experiment. The spatial resolution allows researchers to track the particles that interact within the detector. The energy resolution helps with deducing the mass of the particles through the use of the mass-energy relation. This is increasingly important in rare searches such as for a type of radioactive decay known as neutrino-less double beta decay, $\beta\beta(0\nu)$. Detecting this would prove that the neutrino is its own antiparticle, which would have major implications on the Majorana vs. Dirac nature of neutrinos, the baryon asymmetry problem, and the neutrino mass. Finding that the neutrino is a Majorana particle vs. a Dirac particle would provide a case for lepton violation which was is not allowed under Dirac models [1]. The baryon asymmetry problem is the observation that we live in a matter dominated world without an equal amount of antimatter. If the neutrino is a Majorana particle then heavier neutrino Majorana particles could explain this discrepancy through baryogenesis via leptogenesis [1]. The ability to provide insight into these fundamental questions is why the search for $\beta\beta(0\nu)$ is crucial. To conduct this search, energy resolution in detectors must be drastically improved. The method explored in this paper improves energy resolution in TPC detectors via counting individual primary ionization electrons with the use of electronegative gases.

2 Background

2.1 Energy Resolution

The theoretical limit of $< 1\%$ energy resolution was derived over a decade ago in the context of the $\beta\beta(0\nu)$ search by Dr. David Nygren utilizing the proposed idea of electron counting [6]. The reason why energy resolution is so crucial for the $\beta\beta(0\nu)$ search is due to the two significant backgrounds that the experiments must discriminate against. One being the much more common process of two neutrino beta decay, $\beta\beta(2\nu)$ (seen in Equation 1), and the other being gamma rays and beta particles. $\beta\beta(2\nu)$ produces four particles (two electrons and two neutrinos) that have a total energy, Q. However, only the electrons can be measured by the detector. Figure 1 shows the energy spectrum, blue line, of $\beta\beta(2\nu)$ which is the energy of the two electrons added together. There is a maximum at Q which occurs when the two neutrinos are produced close to rest. The $\beta\beta(0\nu)$ event, however, only produces two electrons which have total energy Q. An energy spectrum can be created from these electron energies like in Figure 1, red line, located at Q. The spectra are made using an energy resolution of 1%. Also, the $\beta\beta(2\nu)$ event rate is set at 100 times that of the $\beta\beta(0\nu)$ event rate which is purely for illustrative purposes. In reality the red peak would be significantly harder to resolve from the blue spectrum which explains why energy resolution is critical.

$$ {}^{A}_{Z}X \longrightarrow {}^{A}_{Z+2}X + 2e^{-} + 2\overline{\nu}_{e} \tag{1} $$

The current experiments with electron drift TPCs have only managed to achieve $\sim$10% energy resolution which is an order of magnitude worse than the theoretical limit mentioned previously. This result is found by analyzing the spectrum of voltage peaks, like in Figure 8, at the readout. This spectrum is gaussian, and the resolution will be described by the σ/μ of this gaussian. To achieve the $< 1\%$ energy resolution required to detect the rare $\beta\beta(0\nu)$ events, Nygren proposed a method of counting individual primary ionization electrons in the detector as I mentioned above. I will go into more detail about this throughout the paper, but the motivation behind this method has to do with how events are produced in a TPC. Each of the electrons produced by the double beta decay event travel through the gas depositing energy through collisions and thus ionizing electrons. The number of ionized electrons is well understood and in perfect conditions follows a Poissonian distribution. Due to each of these ionized electrons contains a fraction of the original energy if you count all of them you can reconstruct the original energy within some Poissonian error. The way this differs from the previous approach of just analyzing the total energy that hit the readout is that this Poissonian distribution makes our energy resolution scale according to $\sim 1/\sqrt{N}$ with N being the number of primary ionization electrons. Now in an event such as $\beta\beta(0\nu)$ N is sufficiently large, $\sim 1 * 10^5$ electrons in Xenon, to improve this energy resolution to $< 1\%$ [6].

2.2 Time Projection Chambers

The TPC was invented by Dr. David Nygren in 1974 [5]. To present an example of one of these detectors I will describe our 60 cm cylindrical detector as can be seen in Figure 2. It consists of an interaction volume that contains the medium of interest (gas mixtures

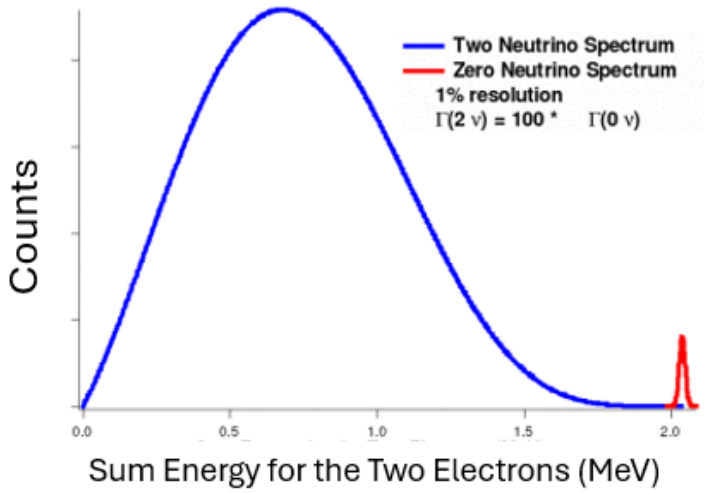

Figure 1: Double beta decay spectrum with the two neutrino spectrum being 100 times the zero neutrino spectrum. The zero neutrino spectrum has a 1% energy resolution. [2]

in our case). This volume is bounded on two sides by a cathode and a grounding plane where an electric field is established along the drift axis. The cathode can be brought to voltages as high as -60 kV. The grounding plane provides the housing for the amplification and readout mechanism. To keep this electric field uniform, the vessel is lined with a field cage. An ionization source is then introduced to our detector whether that is a UV laser (N_2 at 337.1 nm) ionizing electrons from the cathode via the photoelectric effect, or an Fe-55 X-ray source. The Fe-55 is the important source to focus on as it produces a 5.9 keV electron recoil, which, in pure CF_4, ionizes 172 primary ionization electrons, on average. This value is obtained by experimentally measuring the average energy it takes to produce a single ion-pair (the W-value) in the gas, which will be discussed further later in the paper. These electrons then drift through the TPC to a gas electron multiplier (GEM) where each individual electron is amplified by undergoing an electron avalanche process. The GEM has an electric field established across it which forces the electrons through small holes in the GEM where the field is strong enough to produce Townsend avalanching [7]. The signal produced in the avalanche is detected using a preamplifier connected to the bottom electrode of the GEM. The resulting preamplifier signal is digitized using a Tektronix TDS 3054C digital oscilloscope and sent to a data acquisition (DAQ) computer via ethernet. The DAQ system on the computer was developed by a former graduate student in Dr. Loomba's lab, and it consists of taking captures of the oscilloscope readout.

Figure 2 also shows a resulting waveform acquired in a pure CF_4 gas run. The important thing to note in this waveform is that CF_4 is an electron drift gas which means that CF_4 does not easily capture electrons at the low drift fields we are utilizing. Our research has shown, however, that at higher drift fields CF_4 exhibits negative ion drift behavior. The drift velocity is a couple orders of magnitude higher in electron drift compared to negative ion drift, so all of the electrons arrived to the readout in quick succession causing the sharpness of this peak. Since we want to count each electron, the drift velocity needs to be reduced. One method to do this is the introduction of electronegative gases into the interaction volume,

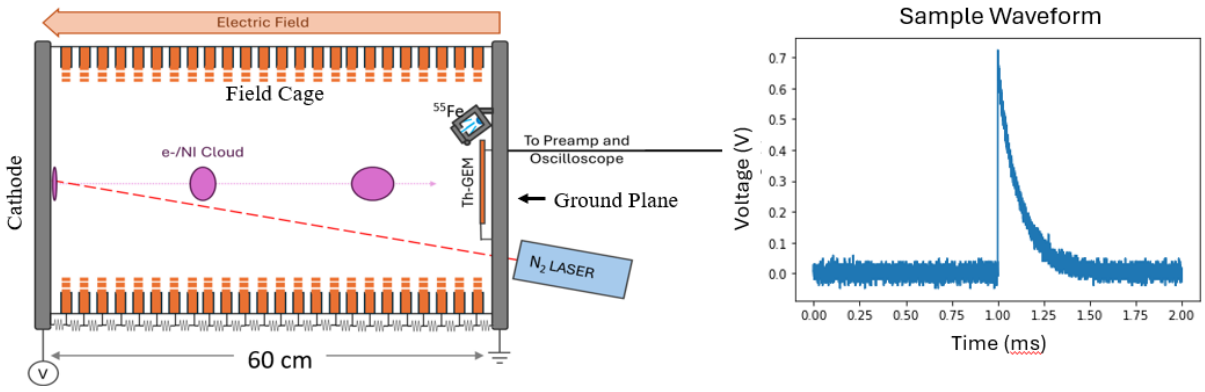

Figure 2: Example of a TPC detector and a sample CF_4 waveform.

which have the property that the molecules will capture the electrons forming an anion. The newly formed anion is much more massive than a single electron thus it drifts slower in TPC's electric field. By slowing down the drift velocity of these charges the arrival time of individual primary ionization electrons on the readout plane will spread out enough that you could detect and count each electron as it arrives.

2.3 Sorensen's Work

A paper published by Dr. Peter Sorensen's group has shown that this electron counting method could be effective in counting each individual primary electron in the event, which could lead to the theoretical $< 1\%$ energy resolution [4]. In their experiment they used a TPC filled to $p = 0.25$ bar with argon (66%), carbon dioxide (30%), and oxygen (4%), the latter being the electronegative gas [4]. This specific gas mixture was used as maximizing the amount of noble gases is important for comparing results to rare event searches. These experiments use noble gases as a target due to their low reactivity, but they are unstable in TPCs so CO_2 is added to stabilize the mixture. This experiment used an Fe-55 source that produces low energy mono-energetic electrons (5.9 keV) in the TPC. These electrons deposit their 5.9 keV energy in the gas ionizing 209 electrons on average [4]. The resulting ionization is captured by the electronegative molecules, which drift towards the GEM. The GEM then strips the electron from the O_2 molecule and amplifies the single electrons to many via the Townsend avalanching process to produce a detectable signal, as seen by the distinct steps in Figure 3. It is important to note that the amplification stage has fluctuations in the number of electrons produced across the GEM. These fluctuations are caused by the variable nature of Townsend avalanching. This can be seen in the different step sizes in Figure 3. Each step correlates to an individual electron reaching the readout plane, but the height of each fluctuates according to the number of electrons produced across the GEM. These electrons then drift onto an anode for detection. The anode used for this experiment is a ring anode that has concentric circles with each ring being a separate readout. The inner rings provide the main readout for the experiment with the outermost ring used as a veto. This means that any event that lands on the outermost ring is thrown out due to the possibility that the track extended out of the detection plane and was not fiducialized.

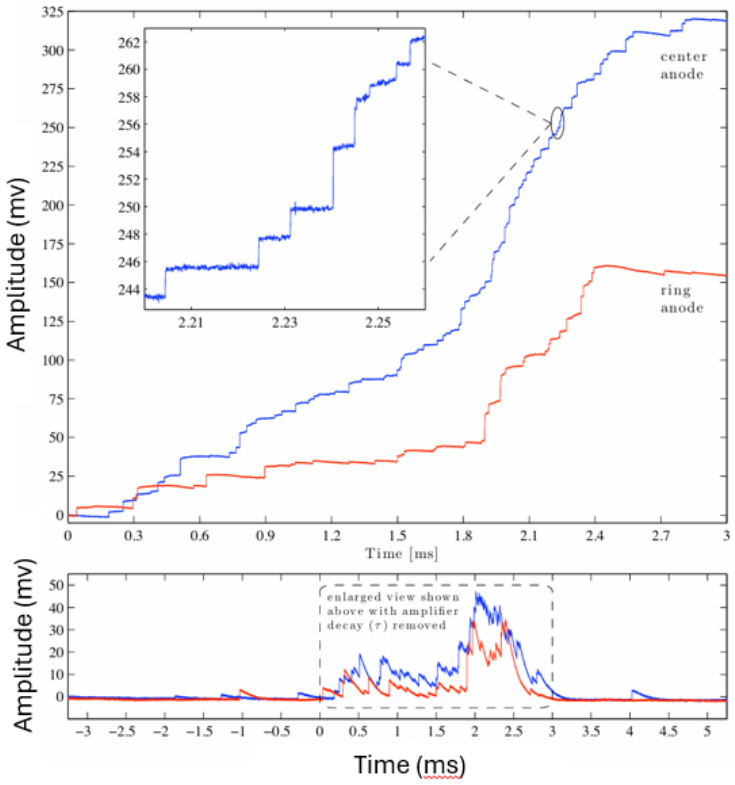

Figure 3: Example 5.9 keV event from the Sorensen experiment. **(Lower)** Event as recorded. **(Upper)** Event with the decay tails removed from each electron to show the steps in voltage from each individual electron. Ref [4]

The group then counted the individual electrons in Figure 3 and created a spectrum of the number of electrons counted in each event. Once they had this spectrum they calculated the energy resolution and got $\sim$ 8% as their best resolution, as seen in Figure 4. While this is an improvement on previous results utilizing electron drift of $\sim$ 10%, it is still quite far from the theoretical limit of $\sim$ 1% for negative ion drift. Sorensen's group provides a few hypotheses as to why they did not reach the theoretical limit, however none of the suggested explanations were tested. After consulting Sorensen we have decided that it could be beneficial to test out other electronegative gases in this experiment, namely CS_2. This gas was chosen as it captures electrons efficiently as well as being easy to strip the electron off the molecule at the GEM. Both O_2 and another electronegative gas SF_6 are harder to strip the electron from.

3 Gas Properties

A crucial precursor to this project was my work with graduate student Elizabeth Tilly on characterizing the gas gain, drift velocity, diffusion, and attachment lengths for various gas mixtures containing noble gases, CS_2, and CF_4. We conducted these experiments in our 60 cm drift length TPC described above, utilizing both an Fe-55 source and a N_2 laser. Gas gain is the average amplification of electrons across the GEM due to the avalanche process.

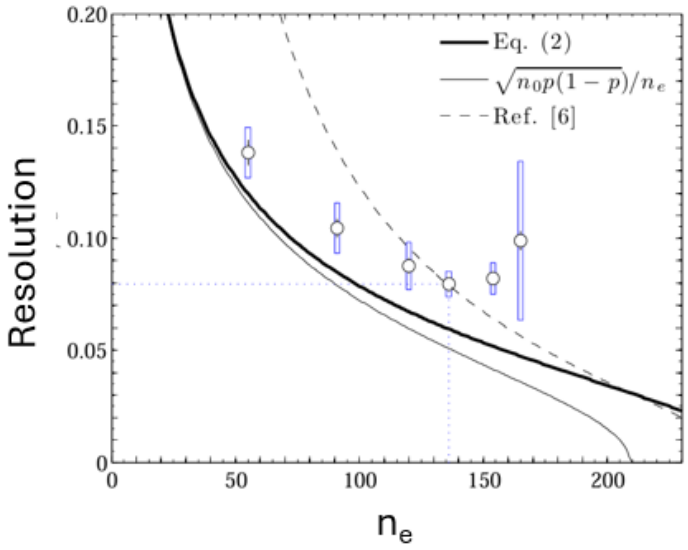

Figure 4: Energy resolution results from the Sorensen experiment with three theoretical limit models discussed in the paper. Eq. 2 is given in the paper. The second model is a binomial process with n_0 being the initial number of ionized electrons, p being the probability an electron is counted, and $n_e = n_0 p$. The third model is from Nygren's initial calculations. Ref [4]

This was measured by comparing the output of electrons from the GEM to the input number of primary ionization electrons (varies with each gas mixture). Drift velocity is measured via the difference in time from the laser firing, which photoionized electrons at the cathode, and their arrival at the readout plane. This describes the average velocity of the electrons or cations drifting through the medium. In the presence of a uniform electric field they should accelerate constantly, however, the electrons and cations will collide with the gas molecules thus slowing them down to an average drift velocity. Diffusion can be measured by converting our voltage readout to a current waveform via equation 2 below. For a negative ion drift mixture the diffusion is found through fitting an exponentially modified gaussian to the current. This is necessary as the attachment length of electrons being captured by the electronegative molecules is evident through an exponential tail on what would otherwise be a gaussian shape. The diffusion is extracted from the sigma of the gaussian piece and attachment is obtained from the exponential piece. The mixture to focus on for the rest of the paper is our 45 torr CF_4 and 5 torr CS_2 mixture. This mixture was chosen for the next sections as we use data from a pure CF_4 run and this will give us a close match while also providing a slight amount of electronegative gas. This also mimics Sorensen's work as they utilized a small fraction of electronegative gas in their mixture. The diffusion and drift velocity data can be seen in Figure 5 for this mixture. A point to note is the minimum in the diffusion plot that is due to the cations in a high electric field diffusing non-thermally. For this work we will only need to look at low electric fields so we can assume thermal diffusion.

$$I(t) \propto \frac{dV(t)}{dt} - \left(-\frac{V(t)}{\tau}\right) \tag{2}$$

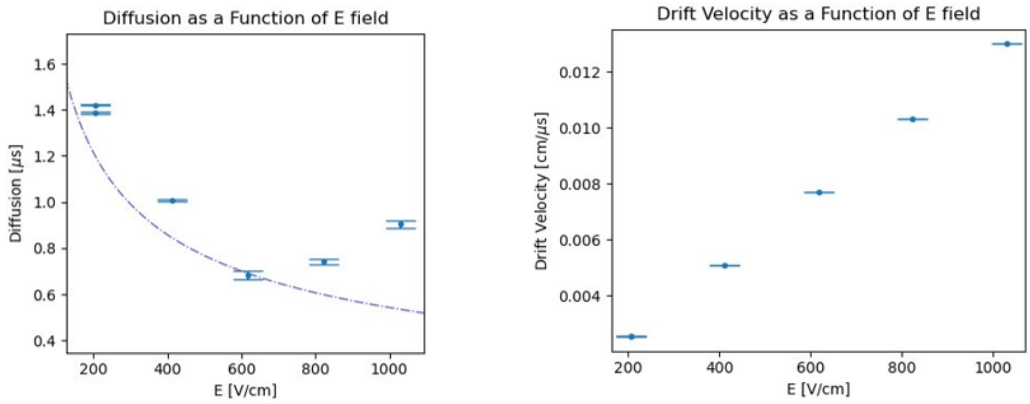

Figure 5: Gas Properties of a 45 torr CF_4 - 5 torr CS_2 mixture. **(Left)** Diffusion as a function of E field after drifting 60 cm with the thermal diffusion curve overlayed. **(Right)** Drift Velocity as a function of E field.

4 Noise Reduction

One of the most important requirements in our experiment is ensuring that the noise in the detector is reduced to an acceptable level so that we can measure the signal from a single electron. We will be conducting the experiment in our box detector which is quite a bit smaller than the previously mentioned cylindrical detector. This TPC will have a drift length of 10 cm compared to the 60 cm described above. We installed an anode similar to the one used in the Sorensen experiment as an initial test. To reduce the noise in our detector we started by only putting in this free floating anode connected to a preamplifier and to our oscilloscope readout. We began by shielding our detector with copper mesh and then moving it into a copper Faraday cage room. This was crucial to reduce most of the noise that we observed as it blocked out any extraneous background sources. To reduce the microphonics, fellow undergraduate student, Stephanie Paiva-Flynn, and I created a suspension system for the detector. Microphonics are where vibrations caused by footsteps, talking, etc. cause a signal in the low frequency range, thus the suspension system helped mitigate this. We also found it was necessary to switch over from a Cremat CR-110-R2.0 preamplifier to an Ortec 142IH preamplifier. This is due to the Cremat preamplifier developing a source of noise that we could not characterize, while the Ortec preamplifier worked as expected. Figure 6 shows the success of our noise reduction efforts where we reduced the noise by two orders of magnitude. The resulting noise is a well behaved gaussian as seen in Figure 7.

5 Simulation

To ensure that the box detector could measure individual electrons as they arrive at the anode, we decided to simulate potential waveforms.

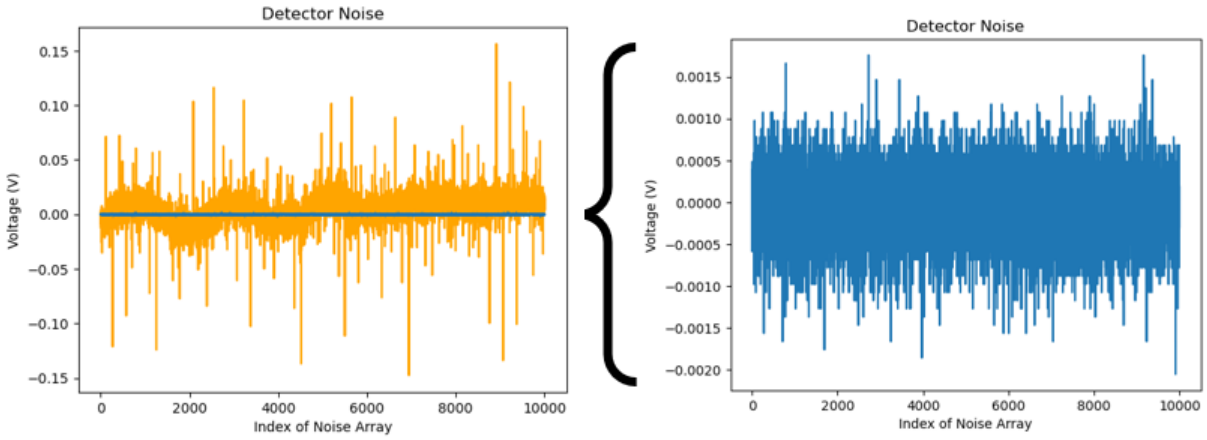

Figure 6: Noise measurements in the box detector taken with a mesh anode. **(Left)** The orange noise measurement was taken before noise reduction, and the blue measurement was taken after. **(Right** Plot of the reduced noise measurment.

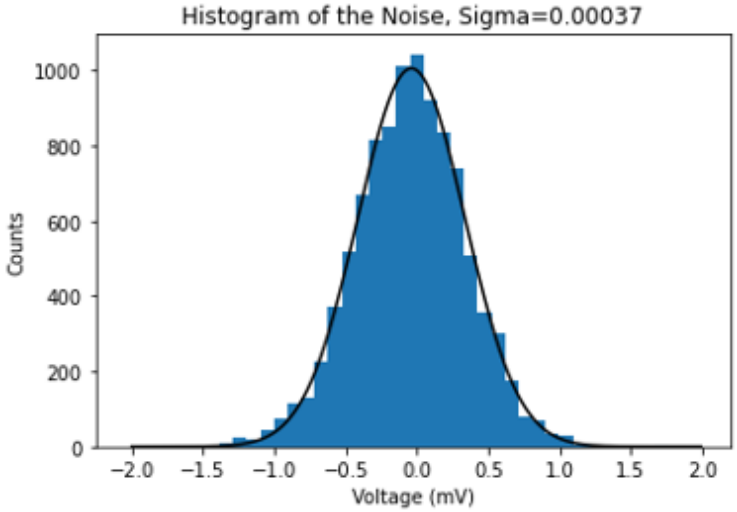

Figure 7: Histogram of the noise after reduction with a gaussian fit.

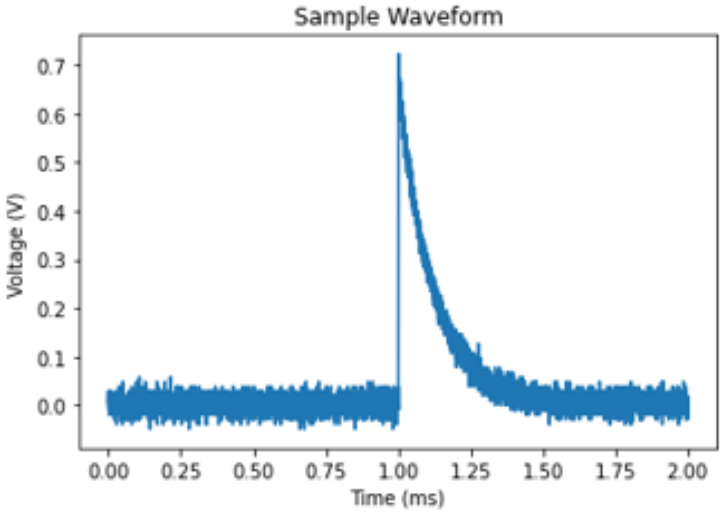

Figure 8: A typical waveform of a 5.9 keV electron event in 50 Torr CF_4 in the cylindrical TPC. This wavefrom consists of 172 electrons.

5.1 Constructing Single Electron Waveforms

To create simulated electron waveforms we first started with real CF_4 waveforms from 5.9 keV electrons produced in the cylindrical detector, as seen in Figure 8. Taking the peak height spectrum and fitting a gaussian to it, a mean was found. This value was then divided by 173, the average number of electrons expected from each event (You might notice I used the number 172 earlier and 173 now; this will become clear shortly). This gives the single electron peak height value of $\mu_e = 4.06$ mV. To find the electron peak fluctuations that we see in Figure 3 we need to look at:

$$R_\infty^2 = W\frac{(F+f)}{E_i} \tag{3}$$

where $R_\infty = \mu_e/\sigma_e$ for one electron; R_∞ being the asymptotic resolution of the detector. We have $W = E_i/n_0$, W being referred to as the W-value, and E_i is the incident particle energy. The W-value describes the mean energy needed to create a single ion pair. Thus when it is divided by the incident energy (5.9 keV in our case) it gives $1/n_0$. The Fano Factor, F, accounts for the fluctuations in the primary ionization, and f is the fractional avalanche variance. Now to utilize equation 3 for a single electron peak we need to focus on f. The peak variation from a single electron will only depend on the variation in its avalanche across the GEM. Taking a calculated minimum value in pure CF_4 of $f = 1.4$, a value obtained from Thorpe and Vahsen [7], we find $\sigma_e = 4.81$ mV.

The rise time and the decay parameter must also be extracted from the real CF_4 waveforms. To find the rise time we take the maximum point of the CF_4 waveforms and the point to the left of that where the waveform reaches zero voltage. We then take this distance for each waveform and average them. This gives us a measured rise time of $\sim 1\mu s$, this is much larger than the theoretical rise time given by the Ortec 142IH documentation (on the order of 50 ns). For the decay tail you fit an exponential to all of the waveforms and average the decay parameter giving you $\tau = 117.53 \pm 1.34\ \mu s$. The decay parameter is less than the

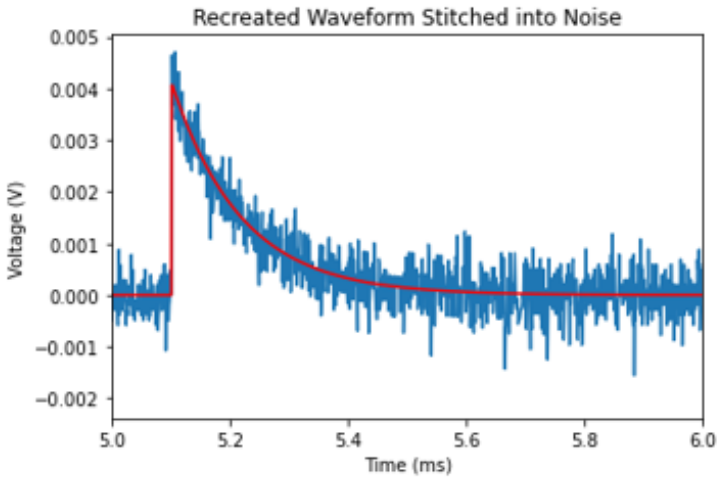

Figure 9: A simulated single electron waveform using parameters obtained from a CF_4 run. The red line is the constructed waveform, and the blue line is that waveform stitched into the box detectors noise.

theoretical result of 200-400 μs given by the documentation.

To then create a simulated single electron waveform we piece together a rise time piece and a decay tail at a height chosen at random from a gaussian distribution with parameters μ_e, σ_e. It must also match the digitization of our noise which is 1 μs. This is then stitched into a real noise waveform, Figure 6 to create a simulated single electron waveform like in Figure 9.

To create a full simulated waveform of 173 electrons we need to stitch 173 of these single electron waveforms together. We take a simulated electron track (from the degrad program[3]), Figure 10, that has 173 primary ionization electrons (this is why we divided by 173 earlier rather than 172). Degrad is a program developed to model primary ionization particle distributions in various gas mixtures [3]. We then apply drift parameters (diffusion and attachment) to this track that match our expected detector operation. This means we apply E = 50 V/cm, v_{drift} = .00075 cm/μs, and diffusion at the thermal limit, 0.317 cm. These parameters are selected by extrapolating the 45 torr CF_4 - 5 torr CS_2 data that I mentioned earlier as this is the closest negative ion dataset that matches our pure CF_4 waveforms used in the construction of the single electron waveforms. This provides us with the timing of when each of the 173 single electron wave forms arrive at the anode giving us a result like Figure 10. This result will vary every time as there are variations in the original track clustering, single electron peak height fluctuations, attachment, and diffusion. To calculate statistically significant results a large number of tracks must be analyzed, however, for the purposes of this paper one track is adequate.

5.2 Walking Average

Detecting the peaks in our fully constructed waveform requires the use of a walking average. This is crucial as it further reduces the noise while highlighting the signal peaks. This is performed by replacing every point with the mean of the previous n points subtracted from the mean of the following n points. The choice of n has some important implications

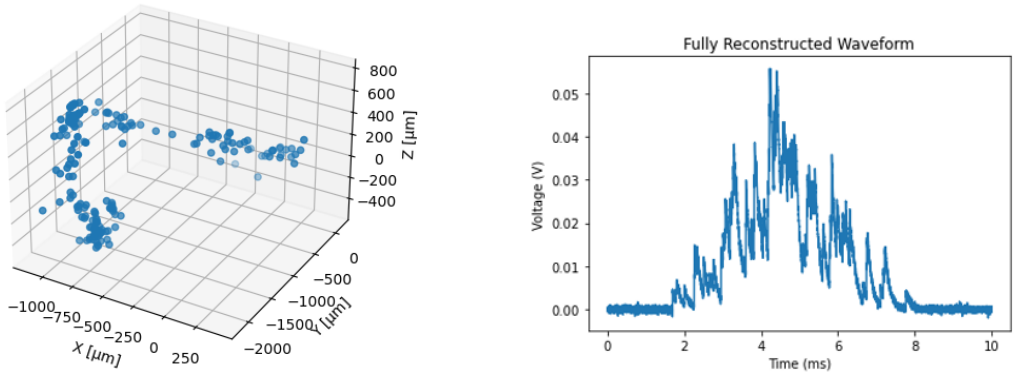

Figure 10: (Left) A simulated 5.0 keV electron event in CF_4 utilizing the degrad program. Axes are in μm [3]. **(Right)** A constructed negative ion drift waveform using the simulated track to find the positioning of each constructed electron event.

as can be seen in Figure 11. As n increases the signal to noise ratio (SNR) of the peaks increases, however, the minimum timing between the peaks arrival must increase for them to be detectable as separate events. This creates a balancing act to pick the right n. For the rest of this paper n=10 is utilized due to it having a high SNR while still having decent time separation as can be seen in Figure 11.

Conducting the walking average on our full waveform yields Figure 12. The peak finding algorithm is then able to find 82/173 possible peaks for this waveform.

5.3 Peak Finding Losses

There are three main reasons why we lose so many peaks. One such reason is due to the electron peak fluctuations. Our peak finding algorithm establishes a 5σ cut above the noise and by comparing that to the gaussian distribution with parameters μ_e, σ_e that we randomly draw peak heights from, we can see that 25% of electrons are lost under this threshold. Our other two reasons can be seen by looking at Figure 13. This figure shows a green line at the 5σ threshold, red x's at the detected peaks, and light red lines at the places where a single electron peak is located. You'll notice from the previous walking average figures, Figure 11 that when performed over many peaks a dip occurs which has caused clearly resolvable peaks to drop below the 5σ threshold also. Now comparing the peaks detected to the true peak locations we can see that many were also lost due to pileup of events. The losses caused by the electron peak fluctuations can be minimized through a higher gain across our GEM, but this is difficult to achieve. The losses caused by the dip are due to the walking average and can be improved by taking a lower value for n. This can also be improved by increasing the sampling rate of the oscilloscope as for the same value of n, the walking average will cover less of the waveform. Any increase would be an improvement, but acquiring a sampling rate around one sample per tens of nanoseconds should drastically improve results. The oscilloscope we currently have is one sample per microsecond at the window size we need. The final cause for losses can also be improved through an oscilloscope with a higher sampling rate, but can also see some improvement through decreasing the drift velocity.

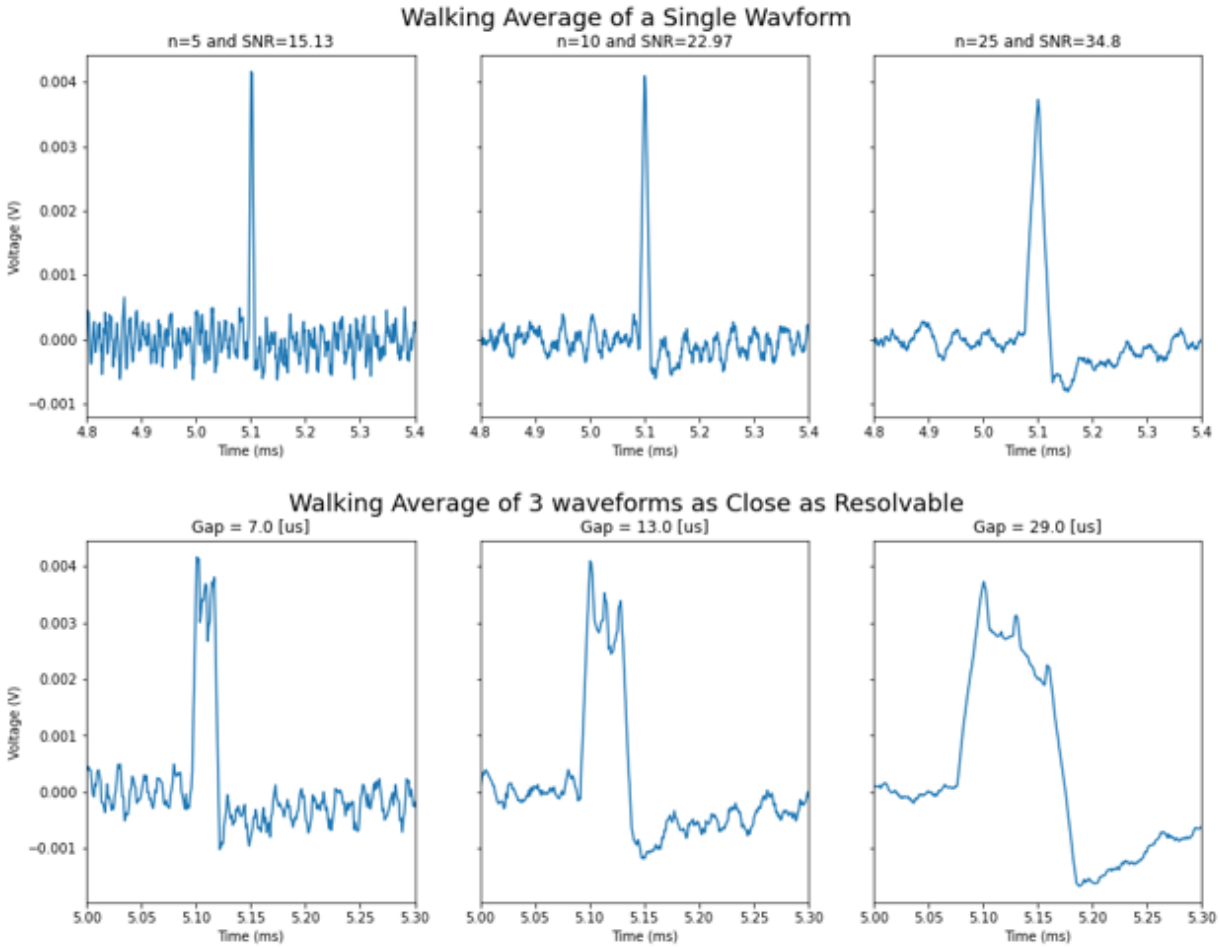

Figure 11: Walking averages comparing different values for n. The left column being n=5, the middle being n=10, and the right being n=25. **(Upper)** These plots show that for one electron peak the signal to noise resolution increases with increasing n. **(Lower)** The plots show three electron peaks placed at their closest time resolvable spacing.

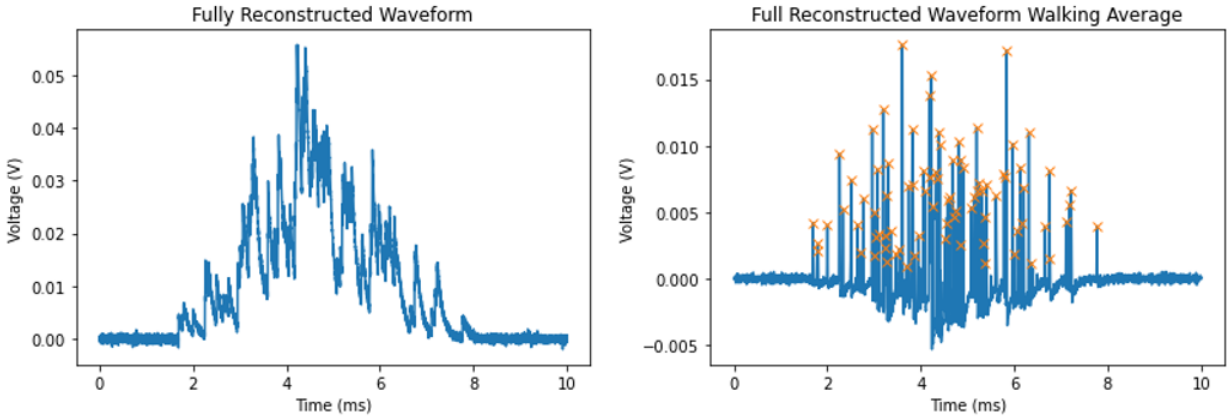

Figure 12: **(Left)** A constructed negative ion drift waveform. **(Right)** The constructed waveform after a walking average with n=10 is performed. The orange x's are where a peak finding algorithm finds peaks above a 5σ threshold above noise.

Figure 13: A zoom in on the reconstructed waveform after the walking average. The green line is the peak finding threshold, the red lines are where the constructed electron tracks are placed in the noise, and the red x's indicate the peaks detected by the peak finding algorithm.

6 Future Work

6.1 Detector Setup

Based on the above analysis, it is clear to see that we will need to setup the detector in a way to minimize the drift velocity. This will ensure the charges arrival at the anode is spread out as much as we can. We will likely use an $Ar/CO_2/CS_2$ mixture in our analysis; the same mixture Sorensen's group used, but with the electronegative gas switched. This allows us to achieve a fairly direct comparison between the two results. This detector will also be operated at a lower electric field further helping to reduce the drift velocity in the TPC and spread out the arrival of the track.

6.2 Hardware Upgrades

For the actual experiment we will need an oscilloscope with a higher sampling rate, as previously established. This should be acquirable through some of our collaborators. Further development on an anode for the experiment will also be necessary. A prototype of the anode has been developed and used in this analysis, but further modifications will need to be made.

7 Conclusion

Improved energy resolution will be crucial to aid in the detection of rare events. Improving energy resolution down towards the theoretical limit will aid in not only the $\beta\beta(0\nu)$ search but potentially dark matter and other rare searches. The method of counting individual primary ionization electrons in a TPC detector has shown to be effective in this goal. With some improvements to our TPC, the previously mentioned anode and oscilloscope with a

higher sampling rate, we will continue the attempts to improve this energy resolution in TPC detectors.

8 Acknowledgments

I would like to thank my advisor, Dr. Dinesh Loomba, for his continuous help over my years of undergraduate research. I would also like to thank Elizabeth Tilly and Stephanie Paiva-Flynn for their direct help with my thesis project. Finally, I would like to acknowledge the funding from the Rayburn Reaching Up Fund, Department of Energy, National Science Foundation, and the University of New Mexico.

References

[1] Evgeny Akhmedov. Majorana neutrinos and other majorana particles:theory and experiment. *arXiv:1412.3320*, 2014.

[2] COBRA Experiment.

[3] Degrad Github Repository, https://fireballpoint1.github.io/GasSimulator/?shellintroduction.

[4] Peter Sorensen et al. Towards energy resolution at the statistical limit from a negative ion time projection chamber. *Nuclear Instruments and Methods in Physics Research Section A: Accelerators, Spectrometers, Detectors and Associated Equipment*, 2012.

[5] David R. Nygren. The time projection chamber: A new 4 pi detector for charged particles. *eConf*, 1974.

[6] David R. Nygren. A negative-ion tpc with ultra-high energy resolution for 0- double beta decay search in ^{136}xe. *Journal of Physics: Conference Series*, 2007.

[7] S.E. Vahsen T.N. Thorpe. Avalanche gain and its effect on energy resolution in gem-based detectors. *Nuclear Instruments and Methods in Physics Research Section A: Accelerators, Spectrometers, Detectors and Associated Equipment*, 2023.